A WALL INTERFERENCE ASSESSMENT/CORRECTION INTERFACE MEASUREMENT SYSTEM for the NASA-ARC 12-FT PWT

Final Memorandum Report

Grant No. NAG 2-551

July 31, 1989

The University of Tennessee-Calspan

Center for Aerospace Research (CAR)

TABLE of CONTENTS

List of Tables

List of Figures

SECTION 1

INTRODUCTION

Wind tunnel wall interference has been recognized as a potential source of error in aerodynamic testing almost since the first wind tunnel data were obtained. Traditional methods for determining the wall interference have been based on linear superposition theories and have been found to be deficient when significant wall interference is present. Advances in the early 1970's provided a new impetus to wall interference theory. New insights were gained in the understanding and treatment of wall interference through the adaptive wall concept. The adaptive wall concept was revolutionary in that it clearly established that a wealth of information about wall interference is contained in the distribution of flow variables measured at, or near, the tunnel boundaries. This insight spawned methods for wall interference assessment/correction (WIAC) techniques that could be applied to any wind tunnel, either with adaptive or passive wall.

The restoration of the NASA Ames Research Center 12-FT Pressure Wind Tunnel (PWT) presents the opportunity to provide a modern test section with a fully integrated WIAC system. The ability to identify and correct for the wall interference in this national high Reynolds number, low speed facility will provide unparalleled high quality experimental results.

An integrated WIAC system is comprised of four components. First, an interface measurement system (IMS) is required to measure the distribution of flow variables, usually pressure and flow angle, on or near the test section walls. For a solid wall wind tunnel like the PWT, the IMS is generally a strategic distribution of static pressure orifices mounted in the tunnel wall since the flow angle is zero at the wall. Second, a data acquisition and processing system is required to capture the data from the IMS. The components of the acquisition and processing system are signal processors for the output of the IMS measurement devices, a data buffer, and a computer (either stand-alone or test integrated) to process the IMS data. Third, WIAC methodology and software are required to determine the wall interference in the tunnel from the processed IMS data. Finally, the output from the WIAC software must be interfaced with either the facility data acquisition computer to provide wall interference corrections to the tabulated data or with the tunnel control system to adjust the tunnel flow conditions to account for the wall interference, or both.

In this first phase of the development of a WIAC system for the PWT, the University of Tennessee-Calspan Center for Aerospace Research (CAR) has developed the design criteria for the IMS. This was accomplished in three primary steps. First, the operational scenarios of the PWT were analyzed as to their requirements for the WIAC system. Secondly, appropriate wall interference theories were evaluated against the requirements determined from the operational scenarios. Finally, the free-air flow about representative models in the PWT was calculated and, specifically, the pressure signature at the location of the tunnel wall was obtained. The number and location of static pressure orifices to adequately describe the pressure signature on the wall were determined. This report presents the results of this development.

SECTION 2

OPERATING SCENARIO

TUNNEL TEST ENVIRONMENT

The PWT will be capable of testing a variety of model configurations mounted from various support systems in a wide range of test types. The model configurations include conventional three-dimensional air vehicles (with or without power), half models or semispan wings, two-dimensional lifting surfaces, air vehicle components such as engine nacelles (with or without power) and air vehicle propulsion systems.

There are five basic support systems. A high speed conventional sting support system can be used for model pitch and roll control. A floor-mounted turntable with pitch control can be used to support half models and semispan wings . A bi-pod strut support can provide pitch and yaw control for large model forces. A high-alpha support provides pitch and yaw control for model pitch angles up to 93 degrees. Finally, a thru-support provides pitch control for two-dimensional lifting models and other special configurations. Additionally, special test configurations are certain to appear that will require some other support arrangement than those described above.

The testing environment immediately after the PWT restoration is complete can now be identified with reasonable certainty. About 50 percent of the testing will be high-alpha aerodynamics. About 25 percent of the testing will be high lift development. The remaining 25 percent will be mostly generic body shape aerodynamic development and generic research. The high alpha and

high lift tests will involve mostly semispan or half models with chord lengths as large as 2 feet and wing spans that extend to 80 percent of the test section diameter. The models will be large to maximize Reynolds number and could easily approach 5 percent solid blockage. Half model fuselage sections will approach 20 feet in length. Semispan and half models will be mounted in the test section either directly to the floor turntable or to a splitter plate for boundary layer control. The major test objective for this family of model/test configurations will be to determine maximum lift coefficient. Sting support and high-alpha support models will be both fighter (low-aspect-ratio) and commercial (high-aspect-ratio) aircraft types. These models will also be large (blockages up to 2 percent) at very high pitch angles with large wakes. Test objectives for these model/test configurations will be aerodynamic performance including high-alpha maneuvering characteristics.

There will probably be a significant amount of testing with both yawed and rolled models. There will be two-dimensional testing in the PWT, but not early after the restoration completion. It should be noted that although the test model may be two-dimensional, the actual tunnel flow will never be two-dimensional because of the cross-sectional shape of the test section.

There will be tests of propellers and propfans. The tests will be for the propulsive devices alone, or for powered nacelles, wings or models.

The operational environment of the tunnel will be adverse. The test section will be on a turntable that rotates toward several access points. Personnel will frequently be walking on the test section floor. Models and test hardware will be rolled into the test section on dollies. The circuit is expected to be very dirty. Dust and other matter will contaminate the flow and tend to collect on the floor.

WIAC INTEGRATION

A WIAC system can be integrated into the test operations in a number of ways. The specific mode in which it is integrated depends on the test environment, the type of test and the objectives of the end user.

The most basic delineation of modes of application is the assessment versus the correction mode. In the assessment mode the WIAC system monitors the IMS data during testing and identifies the presence of wall interference. The integrity of the data is subsequently evaluated. The correction mode goes a step further

by relating the boundary perturbations to interference effects on the model itself and by applying the requisite corrections to the model data, or defining equivalent test conditions.

Data corrections can be applied either globally or locally. The global correction technique determines equivalent free air conditions to which the wind tunnel data correspond. These corrections are normally in the form of Mach number and angles-of-attack and yaw adjustments to the actual test conditions. The local correction technique relates the wall boundary interference signature to the distribution of interference along the model surfaces. Corrections are then applied locally as increments to the model pressure distribution. The calculated corrections to the local surface pressure distribution can then be integrated to obtain forces and moments.

A WIAC system can operate in on-line or off-line modes. An off-line system will assess or correct data at some time after acquisition independently from the test conduct. The off-line mode is also referred to as post-test assessment/correction. An on-line mode will provide real time assessment or correction. The data integrity is assessed immediately and corrections can be applied directly to the on-line tabulated data. The advantage of the on-line system is the ability to customize the test in progress. The disadvantage is that the WIAC procedures can slow the test process because of the necessary calculations.

An on-line WIAC system can also be interactive with the tunnel operation. Operating in this mode, the WIAC system can evaluate the data integrity and, if interference is present, adjust the Mach number and/or model attitude as appropriate to acquire the desired test conditions. Residual, or non-spatially uniform, interference effects can then be corrected, if necessary, either on-line or off-line. The interactive mode would operate in a manner similar to that presently used for the PWT with the Sivells and Salmi correction factors (Reference 1).

The ultimate application of a WIAC system in a wind tunnel is envisioned to have the capability to operate in the on-line, interactive mode and to calculate suitable corrections. This system would allow for the highest quality data for critical measurements of lift, drag and pitching moment on high lift wing and aircraft models. Other types of testing would allow for relaxing the requirements of the WIAC system. The approach for determining the design criteria for the IMS for the PWT was to design to the more demanding requirements. The resulting IMS can supply boundary information sufficient for an on-line, interactive, WIAC system.

SECTION 3

THEORY

WIAC techniques generally require knowledge of the distribution of two independent flow variables in the field of the test article (References 2-6). The independent variables may be measured or modeled theoretically. The attention of many recent developments in WIAC theory has been focused on transonic testing in ventilated wind tunnels. There are some significant differences between WIAC applications in solid wall and ventilated wall wind tunnels, and these differences will be emphasized.

For ventilated tunnels, it is customary to discuss the procedures in terms of the number of flow variables actually measured (References 2-6). Thus the classical theoretical methods in which the flow variables are both determined theoretically, namely the model geometry and an idealized ventilated wall boundary characteristic (References 2 and 7), can be categorized as zero-measured variable procedures. One-measured variable procedures (References 8-19) also incorporate a model geometric description, but make use of the distribution of the longitudinal disturbance velocity over an entire interface near the wall and surrounding the model. In practice, the static pressure distribution is actually measured and the linear relation is used to infer the longitudinal disturbance velocity component. A more accurate determination of the longitudinal component of the disturbance velocity from the measured static pressure is discussed by Labrujère (Reference 20).

One category of two-measured variable procedures consists of the measurement of the distribution of one flow variable near the wall and measurement of the pressure distribution on the model (References 2, 21-24). Another two-measured variable procedure consists of the measurement of the distribution of two independent flow variables near the wall (References 2, 11, 20 and 25-28). In linear, subsonic flow, the distributions of the flow variables can be integrated over the interface surface, with suitable weighting, to directly obtain the wall interference corrections. The model description is not required explicitly. However, there is an assumption that the effective model shape (the shape which accounts for all physical phenomena neglected in the equations of motion; e.g. viscous and vortical effects) for the equivalent free-air flow is not significantly different from that for the tunnel flow.

For solid wall tunnels such as the PWT, a different interpretation is possible. One of the flow variables, the disturbance velocity component normal to the wall, is known. Either an assumption can be made that the displacement effect of the boundary layer is negligible and the normal component is zero, or a correction can be applied from boundary layer calculations, whichever is appropriate. Therefore, a one-measured variable method can be applied without any measurement requirement, or similarly, a two-measured variable method can be applied with the measurement of only one flow variable other than the flow angle at the wall. Consequently, a two-measured variable procedure can be applied with only the measurement of the distribution of the static pressure on the solid wall. This provides the second flow variable as well as sufficient information to calculate boundary layer corrections to the flow angle at the wall, if necessary.

With this background, the available 3-D WIAC procedures will be discussed for their potential application to the PWT. One method, developed by Hackett et al. (References 29-31), is difficult to classify in terms of the number of measured variables because only very limited measurements are made of the static pressure on the wall. Therefore, the distributions of flow variables at the wall cannot be integrated accurately enough over the interface surface to obtain corrections. This is overcome by supplementing the limited pressure measurements with a simplified model representation using a few well-chosen singularities. The strengths of the singularities are determined using the wall pressure measurements and the solid wall, zero normal flow boundary condition. For rectangular cross sections, Hackett et al. (References 29-31) use an image singularity system to satisfy the solid wall boundary condition. For the NASA-ARC 40 ft.X 80 ft. cross section, though, Hackett et al. (Reference 30) used a panel method to satisfy the boundary condition. It is anticipated that a panel method can be implemented to satisfy the boundary condition for the PWT cross section. After evaluating the strengths of the singularities, the wall induced interference can be determined and expressed in global terms as Mach number and angle-of-attack corrections. The Hackett method is superior to the standard one-variable, solid wall methods in that the model representation is deduced from actual wall measurements instead of being assumed a priori.

Other methods are due to Ashill and Weeks (References 27 and 28) and Labrujère (Reference 20). They both require a sufficient number of pressure measurements on the wall to adequately describe the distribution of pressure. They are both linear methods and determine global Mach number and angle-of-attack corrections. The wall induced velocities at the model location are calculated by a straightforward weighted integration of the flow variables over the entire interface surface. The detailed definition of the wall pressure distribution allows for the

elimination of the requirement to represent the test article explicitly. It is estimated that the computational requirements of the Hackett, Ashill and Weeks, and Labrujère methods are comparable.

The relative accuracy of the Hackett method with respect to the Ashill and Weeks or the Labrujère complete two-measured variable procedures without model representation has not been investigated. Data that permit comparison do exist in References 19 and 28.

There remains a limitation in the fullest possible usage of the complete two-variable methods in solid wall wind tunnels. The assumption of the linear nature of the wall interference becomes invalid when there are significant gradients in the distribution of the wall induced velocity field over the extent of the test article. Specifically, global corrections to Mach number and angle-of-attack may not be adequate because of the nonlinearly distributed interference effects on the model.

This limitation was addressed by Labrujère et al. (Reference 32) for 2-D flows over high-lift, multi-element airfoil configurations. They found it necessary to reintroduce a model representation in conjunction with the two-measured variable data to formulate an integral equation to determine the local correction to the flow over the model at the test Mach number and angle-of-attack. A panel method was used to obtain the numerical solution to the integral equation. In the course of WIAC development over the next several years, it is possible that corresponding methods may be developed for 3-D flows. Such developments would extend the Hackett and/or Ashill and Weeks/Labrujère methods to a greater range of configurations with fewer limiting assumptions.

Advanced developments like this have been anticipated and are considered in the definition of requirements for the PWT IMS. It is imperative that the static pressure be measured over the entire wall surface so that full usage can be made of available 3-D WIAC procedures, present and future.

SECTION 4

ORIFICE REQUIREMENTS

A systematic investigation was conducted to determine the orifice number and location requirements for the IMS system. First, two test articles were selected to represent the various testing scenarios in the PWT. Then the test article geometries, along

with the test section geometry itself, were numerically modeled. The flowfield about the test article in free-air was calculated and the pressure signature at the location of the test section walls was determined. A curve fit routine was then used to determine the necessary orifice locations to sufficiently describe the wall pressure signature. The details of this investigation are described below.

MODEL SELECTION

Analysis of the PWT operating scenario revealed that a severe wall interference situation will be encountered for the large half models and for the high-lift configurations. These configurations not only will encounter large interference, but will impose large pressure gradients at the wall. Therefore, representations of both of these situations were chosen to investigate the orifice spacing requirements.

The recent history of aircraft development and present and future trends of aircraft technology (References 33 and 34) were studied to select a representative geometry for this investigation. A summary of transport type aircraft geometry parameters is shown in Table 1. A geometry was selected to be representative of the data in Table 1. The basic characteristics of the chosen model are given below.

Aspect ratio = 8
Body length/wing span = 1.15
Average wing thickness ratio = 0.11

Furthermore, experience dictates that the maximum practical wing span of a wind tunnel model will be limited to about 80 percent of the tunnel width. This criterion was used to size the models for the investigation so that the resulting geometries would generate representatively large levels of wall interference and large pressure gradients at the wall location.

A convenient geometry to use for the model fuselage is that of the ONERA M-5 body of revolution. This geometry, which is described in Figure 1, was used for both the half model and the full-span model.

The resulting model geometries are shown in Figures 2 and 3. The full-span model (Figure 2) has a wing semispan of 4.8 feet and a body length of 11 feet. The model is located on the tunnel centerline for the flowfield calculations. The half model (Figure 3) has a semispan of 9.6 feet and a body length of 22 feet. This model is located on the tunnel floor for the flowfield calculations.

FLOWFIELD CALCULATION

The flow about the models was computed for free-air conditions. The distribution of the longitudinal disturbance velocity component was then determined along the test section wall location. The calculations were obtained for a Mach number of 0.6 and a lift coefficient of 0.5 to simulate very demanding test conditions.

The influences of the model fuselage, wing thickness, and lifting effects were calculated separately and combined by superposition to describe the total model flowfield. The fuselage was represented with a discrete source distribution and the wing thickness and lift were represented by spanwise distributions of 3-D doublets and finite-span horseshoe vortices respectively.

The disturbance potential of a slender body (closed on both ends) is described mathematically by :

$$\Phi_\beta = -\frac{U_\infty}{4\pi}\int_a^b \frac{S'(\xi)\,d\xi}{\left[(x-\xi)^2+\beta^2(y^2+z^2)\right]^{\frac{1}{2}}} \tag{1}$$

For the present calculations, a discrete source distribution was used as an approximation to Eq. (1). Therefore, the disturbance potential due to the body is approximated by:

$$\Phi_\beta = -\frac{U_\infty}{4\pi}\sum_{n=1}^{N} \frac{\left|S_n - S_{n-1}\right|}{\left[(x-x_n)^2+\beta^2(y^2+z^2)\right]^{\frac{1}{2}}} \tag{2}$$

Finally, the disturbance velocity in the longitudinal direction can be calculated by:

$$u_\beta = \frac{\partial \Phi_\beta}{\partial x} \tag{3a}$$

or

$$\frac{u_\beta}{U_\infty} = \frac{1}{4\pi}\sum_{n=1}^{N} \frac{(x-x_n)\cdot\left(S_n - S_{n-1}\right)}{\left[(x-x_n)^2+\beta^2\left[(y^2+z^2)\right]\right]^{\frac{3}{2}}} \tag{3b}$$

The disturbance due to the wing thickness can be described in general form by:

$$\Phi_T = x\int_{-bw}^{bw} \frac{K(\eta)\,d\eta}{\left\{x^2+\beta^2\left[(y-\eta)^2+z^2\right]\right\}^{\frac{3}{2}}} \tag{4}$$

Eq (4) can be simplified by assuming that the doublet strength is independent of its spanwise location (i.e. $K(\eta)=K_0$) which yields the following:

$$\Phi_T = x\ K_0 \int_{-bw}^{bw} \frac{d\eta}{\left\{x^2 + \beta^2\left[\left(y-\eta\right)^2 + z^2\right]\right\}^{\frac{3}{2}}} \tag{5}$$

The integral in Eq (5) can be evaluated explicitly. The disturbance velocity in the longitudinal direction due to the wing thickness can then be expressed as:

$$u_T = \frac{\partial \phi T}{\partial x} \tag{6}$$

The doublet strength k_o is given as a function of the wing geometry and the freestream velocity u_∞ according to the equation:

$$k_o = u_\infty \frac{k_1 \cdot \tau \cdot b_w^2}{\pi \cdot AR^2} \tag{7}$$

Combining equations (5), (6), and (7), the dimensionless disturbance velocity due to the wing thickness can be determined by:

$$\frac{u_T}{u_\infty} = \frac{1}{u_\infty} \cdot \frac{\partial \Phi_T}{\partial x} \tag{8}$$

The wing lifting effects were calculated using a finite-span, elliptically-loaded lifting-line representation to obtain the dimensionless disturbance velocity. The method, which was developed originally for an adaptive wall investigation (Reference 35), consists of the summation of the velocity field induced by a set of finite-span horseshoe vortices constructed following the vortex-lattice guidelines of Hough (Reference 36).

Finally, the total flowfield of the model is obtained by superposition of the body, wing thickness and lifting effects by

$$\frac{u}{u_\infty} = \frac{u_B}{u_\infty} + \frac{u_T}{u_\infty} + \frac{u_L}{u_\infty} \tag{9}$$

As mentioned above, the total free air longitudinal disturbance velocity component was calculated over the entire test section wall location. Therefore, the velocity component is a function of the longitudinal coordinate, x, and the angle, θ , in the y-z plane, see Figure 4.

An example of the flowfield calculations is given in Figures 4 through 7 for the centerline-mounted model. The disturbance velocity distribution along the longitudinal direction at an azimuthal location, θ, of 20 degrees is shown in Figure 4. The distribution of the total disturbance velocity component is the superposition of three components expressed in Eq. (8). The longitudinal dimension is nondimensionalized by the wing chord

length with the wing root leading edge station signified as x=0. Similar disturbance signatures for azimuthal locations of 70, 110, and 160 degrees are shown in Figures 5, 6, and 7 respectively.

INTERFACE DESCRIPTION CRITERIA

The flowfield calculations described above yield a continuous distribution of the pressure at the test section wall location, assuming the linear relationship between the pressure and the longitudinal velocity component. The objective is to determine the number and location of discrete measurements required to provide a sufficiently accurate approximation to the pressure distribution at the wall. First, however, it is necessary to establish accuracy criteria for making that evaluation. The criteria must be based on model parameters since the end product of the system is to make corrections to these parameters.

The accuracy of the interface pressure distribution will be affected by two major error sources. One source is from the approximation of a continuous distribution by a limited number of discrete measurements together with a curve fitting routine. The other source is the error of the measurements themselves. It is assumed that the wall static pressure can be measured and converted to coefficient form with an accuracy of ± 0.005. This is a reasonable assumption for modern pressure systems using electronically scanned pressure transducer modules (ESP).

The effects of the error at the interface are evaluated at the model location as follows. If the test section of the PWT is approximated as being circular, the interference on the model may be expressed in terms of modified Bessel functions as

$$u\left(x, r=0, \theta\right) = \sum_{k=0}^{\infty} \sum_{m=0}^{\infty} e^{ikx} e^{im\theta} A_{k,m} \tag{10}$$

where the constant coefficients $A_{k,m}$ are related to the measured velocity error $u(x, R, \theta)$ on the interface. If the interface error is expanded into a similar series form as

$$u\left(x, R, \theta\right) = \sum_{k=0}^{\infty} \sum_{m=0}^{\infty} e^{ikx} e^{im\theta} B_{k,m} I_m(\beta k, R) \tag{11}$$

then the coefficients $A_{k,m}$ may be related to $B_{k,m}$. The ratio of the disturbance velocity at the model to that at the interface, $u(x,0,\theta) / u(x,r,\theta)$, using equations (10) and (11) is of the order

$$\frac{1}{I_m(\beta k, R)} \tag{11a}$$

Therefore the error at the model location is significantly smaller than the measurement error on the interface.

The configuration (number and location) of the wall measurements can be evaluated, then, by considering only criteria at the interface. Specifically, the distribution of the pressure at the wall obtained from curve fitting the discrete measured data must compare with the calculated pressure distribution within the measurement accuracy. This criterion yields model disturbance distributions that are virtually the same within experimental accuracies, both longitudinally and azimuthally.

Representative results of the orifice number and location evaluation are shown in Figures 8 through 11. The signature of the total disturbance velocity along the longitudinal direction at an azimuthal location of 20 degrees is shown by the solid line in Figure 8. The orifice locations are shown as the circular symbols. The disturbance velocity distribution as determined by a curve-fit (Reference 37) through the calculated data at the discrete orifice locations is shown by the dashed line. As seen in Figure 8, the dashed line is overlayed on the solid line except for a very small excursion in the vicinity of orifice location 4. The quadratic mean of the error is also given in the Figure and is very small. Evaluations for azimuthal locations of 70, 110, and 160 degrees are shown in Figures 9, 10, and 11 respectively. As demonstrated in Figures 8 through 11, the selected IMS orifice configuration produces very high fidelity between the actual and fitted disturbance signatures at the wall location.

ORIFICE LOCATION

Using the analysis as described above, a wall orifice arrangement of 200 orifices was selected. The configuration provides acceptable resolution of the model-induced pressure signal at the wall for the model configurations investigated.

The results of this investigation yield an orifice configuration with 8 rows of 25 orifices each. The test section windows and structure were considered for the azimuthal row placement. It should be noted that the optimum orifice locations include longitudinal rows along the centerlines of each of the test section wall flats. A compromise was necessary to preserve the window areas along the flats. The distribution of orifices along each row was determined by the resolution requirements of the pressure signal. The orifice locations are shown in Table 2 and in Figures 2 and 3. The actual azimuthal location of the longitudinal rows should be as close to the flats as the test section structure permits, but sufficiently removed from the flats to avoid local perturbations at the juncture. . Explicit determination of the ocation was not possible since detailed

design drawings were not available. The azimuthal location can be fixed when the final design is established and drawings are available.

COMPARISON WITH EXISTING WIAC and ADAPTIVE WALL INTERFACE MEASUREMENT SYSTEMS

The selection of the static orifice locations for the PWT as described above was made independently of the survey reported in this section. However comparison with other systems around the world is useful and adds credibility to the independent investigation. The survey of existing IMS systems is summarized in Tables 3 to 5.

Information for experimental WIAC investigations performed in passive test sections with ventilated and impermeable walls is presented in Table 3. Information for residual interference WIAC systems for 3-D tests conducted in 2-D flexible, impermeable, adaptive wall test sections is presented in Table 4. Information for adaptive wall systems with a variety of wall control mechanisms for 3-D adaptations is presented in Table 5.

All of the data presented in Tables 3 to 5 for full-span models are assumed to be for flows that are fully 3-D without lateral symmetry. For those published cases where lateral symmetry was assumed, extrapolation in the number of rows has been made and noted.

No attempt was made in the investigations referenced in Tables 3 to 5 to generalize the azimuthal locations of the longitudinal rows of orifices. In each case, the location was chosen as appropriate to the structure of the experiment, the test section and model configurations. The only known systematic investigation to reduce the number of rows of orifices was by NLR (Reference 19). In their calculations, the number of rows was reduced from 24 to 6 (actually from 13 to 4 with lateral symmetry) without an appreciable effect on the corrected results for the two-variable WIAC method (Reference 20).

There is also no generality in the longitudinal distribution of orifices along the rows. The locations generally have been distributed more closely in the immediate vicinity of the test article than either upstream or downstream. No systematic investigations of the effect on the corrections of reducing the number of orifices per row are known.

Accurate interpolation of pressure measurements around the circumference of circular or octagonal cross sections can be made with data at fewer azimuthal locations than around rectangular cross sections. The PWT cross section with flats interrupting the

otherwise circular shape is favorable in this regard. Comparisons of the number of orifice rows between the PWT and existing tunnels are most significant for tunnels with circular or octagonal cross sections and/or interfaces; i.e. to AEDC 1T, DFVLR DAM, RAE Bedford and TU-Berlin TUB(3-D).

The 8 rows of orifices recommended for the PWT are somewhere in the middle of the spread (4 to 24) of the facilities in Tables 3 to 5. Considering those facilities with circular or octagonal cross sections, only the AEDC 1T has more rows (16), but that choice was conservative for initial, specialized adaptive wall applications. Moreover, the AEDC tests (Reference 3) were carried out at high transonic speeds approaching free-stream Mach numbers of one with a very large test article. The AEDC 1T IMS had to accommodate large gradients in the model-induced pressure field on the interface, especially in the neighborhood of the wing tips. NLR began their investigation with 24 rows for a rectangular cross section, but found that a reduction to 6 rows was adequate.

Examination of the number of orifices per row in Tables 3 to 5 shows that only ONERA/CERT T2, NAE, and AEDC 1T with 34, 40, and 40 respectively had a larger number than that recommended for the PWT. The NAE and AEDC tunnels are used for transonic testing with large gradients of model-induced pressure at the interface. It is apparent from the disturbance plot published by Mokry, et al., (Reference 38) that for a transport configuration at M=0.45 and C_l=0.551 a forty percent reduction in the number of orifices from 40 to 24 per row should not compromise the WIAC results significantly if realistic smoothing and interpolation are used.

The conclusion is that the number and location of the orifices selected for the PWT are consistent with those of other IMS operating in the same Mach number range. The wide variety of test article configurations anticipated for the PWT, as well as the requirements for full-model testing (in and out of ground effect) and half-model testing, necessitate more measurements than the minimum numbers found sufficient in the testing reported in the literature. Furthermore, the number and location of the orifices should suffice regardless of the course of future development of two variable nonlinear WIAC methods.

SECTION 5

MEASUREMENT SYSTEM DESIGN

The ultimate integrity of a WIAC system will depend on the accuracy of the measurement of the static pressure at the test section wall. Therefore, a well conceived orifice geometry and measurement system design is vital to the performance of the PWT WIAC system. A large body of experience and knowledge has been gained designing pressure measurement systems for wind tunnel tests at AEDC. This experience has been applied using the methods described in References 39 and 40 to arrive at the following pressure system design criteria.

ORIFICE DESIGN

The orifice geometry is critical to the accurate measurement of the static pressure on the wall surface. Errors can be generated if the hole has burrs, rounded edges, or other imperfections from poor installation or subsequent damage. But even if the hole is constructed perfectly, residual errors can still be significant, especially if the orifices are poorly designed. The residual error is caused by local perturbations to the flow and the resulting disturbance of the boundary layer.

Most of the orifice design development has been accomplished experimentally. Investigators typically assume a zero diameter orifice to have zero error. They then determine the relationship between orifice size and residual error. If the orifice error is non-dimensionalized by the local value of the wall shear stress, then the resulting relationship (Reference 39) is

$$\Delta P = \left(\frac{\tau_w}{\rho} \right)^{\frac{1}{2}} \frac{d}{\upsilon} \tag{12}$$

where ΔP = the static pressure error,
τ_w = wall shear stress,
ρ = the fluid density,
d = the orifice diameter,
and υ = the absolute viscosity.

As can be seen from Eq. (12), the measurement error can be decreased by decreasing the orifice diameter. However, practical problems arise as the orifice diameter gets very small. The

orifices become overly susceptible to contamination and are easily stopped-up. Therefore, the pragmatic orifice size selection is a compromise between a tolerable pressure measurement error and operational considerations. Calculations were made for various values of the above parameters to cover the entire operating range of the PWT. The criterion used to calculate the allowable orifice diameter was to have a pressure error less than 0.1 percent of the measured static pressure. The orifice diameter recommended for the PWT IMS system is 0.020 in. This diameter has been used extensively in wind tunnel test models and in many static pipe and wall orifices at AEDC with great success. Orifices of this diameter are relatively free from contamination problems and have less than 0.1 percent pressure error over the range of flow conditions to be experienced in the PWT.

The pressure measurement error is also a function of the ratio of orifice diameter to the orifice depth. The optimum depth (Reference 40) for the PWT IMS orifices is one-half the diameter. This orifice geometry is very difficult to manufacture, however, and a depth equal to the diameter is recommended as a good compromise. The recommended orifice geometry is shown in Figure 12.

PNEUMATIC TUBING CRITERIA

An analysis of the pressure lag caused by various pneumatic tubing lengths and diameters was conducted with an unpublished pressure lag analysis technique that is commonly used for similar analyses. The recommended tubing diameter is 0.040 in. and the tubing length should not exceed 20 ft. between the orifice and the pressure transducer.

ORIFICE INSTALLATION

The best method for orifice installation is to fabricate the orifice itself in a small plug insert and to install the plug in the test section wall. This method is superior because it allows for a high quality, table machined orifice plug that can be removed and replaced if it becomes damaged. The plug insert should be manufactured in brass. The brass plug inserts are then press fit into holes drilled into the test section wall. The plug face is made flush with the wall by filing and sanding. This orifice installation technique is already familiar to NASA-ARC personnel. The plug geometry is also shown in Figure 12.

Consideration was given to innovative ways to install the orifices in the test section. One method was to install the orifices in metallic strips. The strips could be positioned as

desired, thereby giving a great deal of flexibility to the placement. Another idea was to install the orifices in strips that would then be placed in machined slots in the test section walls. This would allow for metric or non-metric interchangeable strips to be used where needed, again for flexibility. However, it was finally decided to stay with the conventional method of installing the orifices directly in the walls. This is the most reliable method for a production facility and will ultimately be the most trouble-free. The presence of the wall orifices will require operating procedure considerations to protect them from damage by personnel walking over them and rolling or dragging hardware over them. Protective mats or floor covering should be sufficient for orifice protection. It is recommended that the capability of purging the orifices by blowing high pressure air through the the orifices from the transducer side of the pressure tubing be included in the pressure measurement system.

SECTION 6

SUMMARY

Development of modern, complex air vehicle configurations is placing increasing demands on wind tunnel testing capabilities. A major area of concern is wall induced interference. Recent developments in wall interference technology provide a means for assessing and correcting for the wall induced interference using information contained in the distribution of flow variables measured at, or near, the wall. The restoration of the PWT provides an excellent opportunity to incorporate a measurement system with which wall interference assessment/correction technology can be applied. In this first phase of the development of a WIAC system for the PWT, the design criteria for the placement and the geometry of wall static pressure orifices were determined.

The design criteria were developed with a three step approach. First, the operational environment of the PWT was analyzed as to the requirements for the WIAC system. Second, appropriate wall interference theories were evaluated against the the requirements determined from the operational environment. Third, the flow about representative models in the PWT was calculated and, specifically, the pressure signatures at the location of the test section wall were obtained. The number of discrete pressure measurements and their locations were determined by curve fitting the pressure distribution through the discrete measurements and evaluating the resulting error (the RMS difference between the actual pressure distribution and that from the curve fit).

The operational environment of the PWT will be very demanding. Large models to maximize Reynolds number will be commonplace. A varied collection of model support systems will adapt to many different types of models and test configurations. There will be two-dimensional model testing and propulsion testing as well as the variety of conventional model testing. This environment will result in many, varied model induced pressure distributions on the wall. The IMS, then, has to be sufficiently generalized to provide an accurate description of the pressure distribution on the wall for any of these situations.

WIAC procedures require the knowledge of the distribution of two independent parameters of the flow field. These parameters may be either measured or calculated with a theoretical model. The most familiar WIAC procedure is the classical, zero-measured variable method where the model geometry and wall characteristics are determined theoretically. The one-measured variable methods also incorporate a model geometric description, but use the measured distribution of static pressure at the wall location to infer the longitudinal disturbance velocity distribution. There are two types of two-measured variable procedures. One method uses the measurement of a flow variable at, or near, the wall and one at the model. This category is limited for 3D flows because sufficiently detailed pressure data on the model surfaces is rarely obtained. The other type uses the measurement of two flow variables at, or near, the wall.

Application of the one- and two-measured variable methods becomes easier in solid wall tunnels because the normal disturbance velocity at the solid wall is known. Therefore, the one-measured variable methods can be applied with no measurements (if the wall boundary layer is ignored), and the two-measured variable methods can be applied with only one measurement other than the normal disturbance velocity.

All of the WIAC procedures, including foreseeable developments in current technology, were considered for the PWT IMS design. The number and location of the static pressure orifices are sufficient for the application of any of the procedures.

The model configurations chosen to calculate representative disturbance velocity signatures at the wall location were a large centerline, sting-mounted high-lift aircraft and a large floor-mounted half model. These configurations were chosen because of the severe test conditions they imposed within the test section.

The disturbance velocity signatures at the wall location were actually determined by calculating free-air flowfields about the model configurations. The distribution of the disturbance velocity over the entire wall location was then obtained from the flowfield calculations.

The free-air flowfield about the model was a superposition of the individual contributions of the model fuselage blockage and the model wing lift and thickness. The fuselage was represented with a discrete source distribution and the wing thickness and lift were represented with spanwise distributions of 3-D doublets and finite-span horseshoe vortices respectively.

Finally, based on the gradients of the disturbance velocity distribution at the wall location, the number and location of orifices necessary to adequately describe the distribution were selected. The orifice configuration was then evaluated by comparing the actual distribution with that determined from curve-fitting through the discrete orifice locations. Analysis of the ratio of the magnitude of the error in describing the disturbance velocity distribution at the wall to the magnitude of the error at the model location indicated that the criterion for sufficient accuracy is appropriately applied at the wall. This is because the error is much smaller at the model than at the wall. Therefore, a criterion for accuracy for the disturbance velocity description at the wall was developed based on the accuracy of the measurement of the static pressure at the wall, which is ± 0.005 in pressure coefficient. The selected configuration of orifice locations easily satisfies this criterion. The orifice locations were adjusted to not interfere with the test section windows or major structural components.

The resulting orifice number and locations were compared with existing wind tunnels with both adaptive and WIAC capabilities. The PWT IMS compares conservatively with existing systems in that it has about the same number, or more, than those systems. The conservative comparison is good to ensure the generality of the PWT IMS and its applicability to future WIAC developments.

An orifice design and installation technique is also recommended. The orifice design is based on a compromise between minimum pressure error considerations, and pressure lag and durability considerations. The design will provide pressure measurements with less than 0.1 percent error over the PWT operating range and will be relatively free from plugging problems from flow contamination or traffic damage during test modifications. The orifices should be fabricated as brass plug inserts and then press-fitted into the tunnel wall. This allows for high quality orifices that can be removed and replaced if they become damaged. The tubing length between the orifices and the transducers was analyzed for lag considerations. A length not to exceed 20 ft. for 0.040 in. diameter tubing is recommended to minimize pressure lag.

REFERENCES

1. Sivells, J. C. and Salmi, R. M., "Jet-Boundary Corrections for Complete and Semispan Swept Wings in Closed Circular Wind Tunnels," NACA Technical Note 2454, 1951.

2. Kraft, E.M., "An Overview of Approaches and Issues for Wall Interference Assessment/Correction," NASA CP-2319, 1984, pp. 3-20.

3. Kraft, E.M., Ritter, A., and Laster, M.L., "Advances at AEDC in Treating Transonic Wind Tunnel Wall Interference," ICAS Proceedings, 1986, pp. 748-769.

4. Mokry, M., "Residual Interference and Wind Tunnel Wall Adaptation," AIAA-89-0147, Jan. 1989.

5. Newman, P.A., Kemp, W.B., Jr., and Garriz, J.A., "Emerging Technology for Transonic Wind-Tunnel-Wall Interference Assessment and Correction," SAE Technical Paper Series No. 881454, Oct. 1988.

6. Newman, P.A., Kemp, W.B., Jr., and Garriz, J.A., "Wall Interference Assessment and Corrections," NASA CP-3020, Vol. 1, Part 2, 1989, pp. 817-851.

7. Pindzola, M., and Lo, C.F., "Boundary Interference at Subsonic Speeds in Wind Tunnels With Ventilated Walls," AEDC-TR-69-47, May 1969.

8. Capelier, C., Chevallier, J.P., and Bouniol, F., "Nouvelle methode de correction des effets de parois en courant plan," La Recherche Aerospatiale, Jan.-Feb. 1978, pp. 1-11; also translated as ESA-TT-491, Aug. 1978.

9. Mokry, M. and Ohman, L.H., "Application of the Fast Fourier Transform to Two-Dimensional Wind Tunnel Wall Interference," Journal of Aircraft, Vol. 17, No. 6, June 1980, pp. 402-408.

10. Mokry, M. "Subsonic Wall Interference Corrections for Finite-Length Test Sections Using Boundary Pressure Measurements," AGARD-CP-335, May 1982, pp. 10.1-10.15.

11. Smith, J., "Measured Boundary Conditions for 2D Flow," AGARD-CP-335, May 1982, pp. 9.1-9.15.

12. Sawada, H., "A General Correction Method of the Interference in 2-Dimensional Wind Tunnels with Ventilated Walls," Transactions of the Japan Society for Aeronautical and Space Sciences, Vol. 21, No. 52, Aug. 1978, pp. 57-68.

13. Sawada, H., "An Experiment of Lift Interference on 2-Dimensional Wings in a Wind Tunnel with Perforated Walls," Transactions of the Japan Society for Aeronautical and Space Sciences, Vol. 22, No. 58, Feb. 1980, pp. 191-202.

14. Sawada, H., "A New Method of Calculating Corrections for Blockage Effects in Two-Dimensional Wind Tunnel with Ventilated Walls, Using Wall Pressure Measurements," Transactions of the Japan Society for Aeronautical and Space Sciences, Vol. 23, No. 61, Nov. 1980, pp. 155-168.

15. Rizk, M.H. and Smithmeyer, M.G., "Wind Tunnel Interference Corrections for Three-Dimensional Flows," Journal of Aircraft, Vol. 19, No. 6, June 1982, pp.465-472.

16. Rizk, M.H. and Murman, E.M., "Wind Tunnel Wall Interference Corrections for Aircraft Models in the Transonic Regime," Journal of Aircraft, Vol. 21, No. 1, Jan. 1984, pp.54-61.

17. Rizk, M.H., "Improvements in Code TUNCOR for Calculating Wall Interference Corrections in the Transonic Regime," AEDC-TR-86-6, March 1986.

18. Sickles, W.L. and Erickson, J.C., Jr., "Evaluation of Wall Interference Assessment and Correction Techniques," AEDC-TR-87-45, June 1988.

19. Maarsingh, R.A., Labrujère E., and Smith, J., "Accuracy of Various Wall-Correction Methods for 3D Subsonic Wind Tunnel Testing," AGARD-CP-429, Sept. 1987, pp. 17.1-17.13.

20. Labrujère T.E., "Correction for Wall-Interference by Means of a Measured-Boundary-Condition Method," NLR TR 84114 U, Nov. 1984.

21. Kemp, W.B., Jr., "Toward the Correctable-Interference Transonic Wind Tunnel," AIAA-76-1794CP, June 1976.

22. Kemp, W.B., Jr., "Transonic Assessment of Two-Dimensional Wind Tunnel Wall Interference Using Measured Wall Pressures," NASA CP-2045, Vol.1, Part 2, March 1978, pp. 473-486.

23. Kemp, W.B., Jr. and Adcock, J.B., "Combined Four-Wall Interference Assessment in Two-Dimensional Airfoil Tests," AIAA Journal, Vol. 21, No.10, Oct. 1983, pp.1353-1359.

24. Murman, E.M., "A Correction Method for Transonic Wind Tunnel Wall Interference," AIAA-79-1533, July 1979.

25. Lo, C.F. and Kraft, E.M., "Convergence of the Adaptive-Wall Wind Tunnel," AIAA Journal, Vol. 16, No. 1, Jan. 1978, pp. 67-72.

26. Kraft, E.M. and Dahm, W.J.A., "Direct Assessment of Wall Interference in a Two-Dimensional Subsonic Wind Tunnel," AIAA-82-0187, Jan. 1982.

27. Ashill, P.R. and Weeks, D.J., "A Method for Determining Wall-Interference Corrections in Solid-Wall Tunnels from Measurements of Static Pressure at the Walls," AGARD-CP-335, May 1982, pp.1.1-1.12.

28. Ashill, P.R. and Keating, R.F.A., "Calculation of Tunnel Wall Interference from Wall-Pressure Measurements," Journal of the Royal Aeronautical Society, Vol. 92, NO. 911, Jan. 1988, pp. 36-53.

29. Hackett, J.E., "Living With Solid-Walled Tunnels," AIAA Paper No. 82-0583, March 1982.

30. Hackett, J.E., Sampath, S., and Phillips, C.G., "Determination of Wind Tunnel Constraint Effects by a Unified Wall Pressure Signature Method: Part 1, Applications to Winged Configurations," NASA CR-166186, June 1981.

31. Hackett, J.E., Sampath, S., Phillips, C.G., and White, R.B., "Determination of Wind Tunnel Constraint Effects by a Unified Wall Pressure Signature Method: Part II, Application to Jet-in-a-Crossflow Cases, NASA CR-166187, Nov. 1981.

32. Labrujère, T.E., Maarsingh, R.A., and Smith, J., "Wind Tunnel Wall Influence Considering Two-Dimensional High Lift Configurations," Journal of Aircraft, Vol. 23, No. 2, Feb. 1986, pp. 118-125.

33. Taylor, J.W.R., Editor, "Jane's All the World's Aircraft, 1988-89," Jane's Information Group Ltd., Coulsdon, U.K., 1988.

34. Nicolai, L.M., "Fundamentals of Aircraft Design," Mets, Inc., Xenia, Ohio, 1975.

35. Erickson, J.C., Jr., "Application of the Adaptive-Wall Concept to Three-Dimensional Low-Speed Wind Tunnels," NASA CR-137917, Sept. 1976.

36. Hough, G.R., "Remarks on Vortex-Lattice Methods," Journal of Aircraft, Vol. 10, No. 5, May 1973, pp. 314-317.

37. Akima, H., "A Method of Smooth Curve Fitting," ESSA Technical Report ERL 101-ITS 73, Jan. 1969.

38. Mokry, M., Digney, J.R., and Poole, R.J.D., "Doublet-Panel Method for Half-Model Wind Tunnel Corrections," Journal of Aircraft, Vol. 24, No. 5, May 1987, pp. 322-327.

39. Franklin, R.E. and Wallace, J.R., "Absolute Measurements of Static-Hole Error Using Flush Transducers," Journal of Fluid Mechanics, Vol. 42, Part 1, Aug. 1969, pp.33-48.

40. Shaw, R., "The Influence of Hole Dimensions on Static Pressure Measurements," Journal of Fluid Mechanics, Vol. 7, March 1960, pp.550-564.

41. Mokry, M., "Subsonic Wall Interference Corrections for Half-Model Tests Using Sparse Wall Pressure Data," National Research Council of Canada, Ottawa, Aeronautical Rept. LR-616, 1985.

42. Wedemeyer, E. and Lamarche, L., "The Use of 2-D Adaptive Wall Test Sections for 3-D Flows," AIAA 15th Aerodynamic Testing Conference, San Diego, Cal., May 18-20, 1988, pp. 331-340, Paper No. 88-2037CP.

43. Rebstock, R. and Lee, E.E., Jr., "Capabilities of Wind Tunnels With Two Adaptive Walls to Minimize Boundary Interference in 3-D Model Testing," Transonic Symposium, NASA Langley, NASA CR-3020, Vol. 1, Part 2, April 1988, pp. 891-910.

44. Archambaud, J.P. and Mignosi, A., "Two-Dimensional and Three-Dimensional Adaptation at the T2 Transonic Wind Tunnel of ONERA/CERT," AIAA 15th Aerodynamic Testing Conference, San Diego, Cal., May 18-20, 1988, pp. 342-350, Paper No. 88-2038CP.

45. Lewis, M.C., Neal, G. and Goodyer, M.J., "Adaptive Wall Research with Two- and Three-Dimensional Models in Low Speed and Transonic Tunnels," AIAA 15th Aerodynamic Testing Conference, San Diego, Cal., May 18-20, 1988, pp. 331-340, Paper No. 88-2037CP.

46. Lee, D.C.L. and Sears, W.R., "Experiments with an Adaptive-Wall Wind Tunnel for Large Lift," Journal of Aircraft, Vol. 24, No. 6, June 1987, pp. 371-376.

47. Sears, W.R. and Lee, D.C.L., "Experiments in an Adaptive-Wall Wind Tunnel for V/STOL Testing," AFOSR-86-2088TR, Sept. 1986.

48. Ganzer, U., "A Short Note on Recent Advances in the Adaptive Wall Technique for 3D-Model Tests at the TU-Berlin," AGARD-CP-348, Feb. 1984.

49. Ganzer, U., Igeta, Y., and Ziemann, J., "Design and Operation of TU-Berlin Wind Tunnel with Adaptive Walls," ICAS Prceedings 1984, pp. 52-65.

50. Ganzer, U., "A Review of Adaptive Wall Wind Tunnels," Progress in Aerospace Sciences, Vol. 22, Pergamon Press, 1985, pp. 81-111.

51. Rebstock, R., "Verfahren zur Berechnung Transsonischer Stromungen fur die Regelung Adaptiver Windkanale," Dissertation, TU-Berlin, March 1986; translated as NASA TM-88530, January 1987.

52. Wedemeyer, E., Heddergott, A., and Kuczka, D., "Deformable Adaptive Wall Test Section for Three-Dimensional Wind Tunnel Testing," Journal of Aircraft, Vol. 22, No. 12, Dec. 1985, pp. 1085-1091.

53. Heddergott, A., Kuczka, D., and Wedemeyer, E., "The Adaptive Rubber Tube Test Section of the DFVLR Goettingen," Paper presented at the 11th International Congress on Instrumentation in Aerospace Simulation Facilities, Stanford, CA., In: ICIASF '85 RECORD, IEEE publ. 85CH2210-3, 1985, pp. 154-164.

54. Heddergott, A., and Wedemeyer, E., "Some New Test Results in the Adaptive Rubber Tube Test Section of the DFVLR Goettingen," ICAS Proceedings, 1988, Vol. 2, pp.1172-1180.

55. Schairer, E.T., "Experiments in a Three-Dimensional Adaptive-Wall Wind Tunnel," NASA TP-2210, Sept. 1983.

56. Whitfield, J.D., Jacocks, J.L., Dietz, W.E., and Pate, S.R., "Demonstration of the Adaptive Wall Concept Applied to an Automotive Wind Tunnel," SAE Paper 820373, Feb. 1982; also AIAA 82-0584, March 1982.

TABLE 1

Characteristic Transport Aircraft Geometry

AIRCRAFT	BODY LENGTH / WING SPAN	ASPECT RATIO	AVERAGE THICKNESS RATIO
737-200	1.04	8.8	12.89
747-200	1.15	7.0	13.4(IN) 7.8(MID) 8.0(OUT)
757-200	1.23	7.8	---
767-200	0.99	7.9	15.1(ROOT) 10.3(TIP)
C-5	1.04	7.75	12
MD-80	1.26	9.62	11
DC-10	1.03	7.5	12.2(ROOT) 8.4(TIP)
MD-11	1.14	7.5	---

Reference 33

TABLE 2

Orifice Locations

ORIFICE NUMBER	TUNNEL STATION FT
1	0.0
2	2.4
3	4.8
4	7.2
5	9.6
6	12.0
7	14.4
8	15.4
9	16.4
10	17.4
11	18.4
12	19.4
13	20.4
14	21.4
15	22.4
16	23.4
17	24.4
18	25.4
19	26.4
20	27.4
21	28.4
22	29.4
23	30.4
24	31.4
25	32.4

ORIFICE ROW	AZIMUTHAL ANGLE Θ,Deg.
A	20
B	70
C	110
D	160
E	200
F	250
G	290
H	340

See also Figures 2 and 3

Table 3

WIAC Systems – 3D Passive-Wall Tunnels

					NUMBER OF INTERFACE MEASUREMENTS: # Longitudinal Rows x # Orifices Per Row				
					Full Model		Half Model		
ORGANIZATION	TUNNELS	CROSS SECTION	TEST REGIME	WALL CONFIG	CONFIGURATIONS	NUMBERS	CONFIGURATIONS	NUMBERS	REF.
Lockheed, GA. Marietta,GA.	30inx 42in 16ftx23ft	R	Low Speed High Lift& Blockage	I	Simple Bluff Bodies Jet-Flap Wing	(1) 4x20=80 8x20=160	Simple Wings Jets in CrossFlow	3x20=60	29-31
NAE/NRC Ottawa, Ont. Canada	5ftx5ft	S	Transonic High Lift	P	Wing/Fuselage, Slender Rocket Launcher	4x40=160	Transport Wing/Fuselage	(2) 6x40=240	10,38,41
NLR Amsterdam, Netherlands	MT(.8mx.6) LST(3mx2.25m)	R R	Low Speed, High Lift	I	Flapped Wing/Fuselage/ Tail	(3) 24x22=528	-No Tests -		19
RAE/Bedford U.K.	13ftx9ft	O	Low Speed, High Lift & Blockage	I	-No Tests -		Flat Plates, Fighter, Jet in Crossflow	(4) 7x15=100	28

R - Rectangular
S - Square
O - Octangular

I - Impermeable, Planar Walls
P - Perforated Walls

(1) - Extrapolated from laterally-symmetrical case, where 3x20 and 5x20 were used, respectively.
(2) - Increased from 4x40 in initial tests.
(3) - Extrapolated from laterally-symmetrical case, where 13x22 were used.
(4) - Some rows have more than 15, some have less, for a total of 100.

Table 4

WIAC Systems – 3D Testing in 2D Adaptive-Wall Tunnels

					NUMBER OF INTERFACE MEASUREMENTS: # Longitudinal Rows x # Orifices Per Row				
					Full Model		Half Model		
ORGANIZATION	TUNNELS	CROSS SECTION	TEST REGIME	WALL CONFIG	CONFIGURATIONS	NUMBERS	CONFIGURATIONS	NUMBERS	REF.
DFVLR Goettingen,FRG	HKG	R	Transonic	FI	Axisymmetric Body, Wing/Fuselage	2x24 + 10x18=228	- No Tests -		42
NASA/LaRC Hampton, VA.	TCT	S	Transonic	FI	- No Tests -		Unswept Tapered Wing	7x18=126	43
ONERA/CERT Toulouse, France	T2	R	Transonic	FI	Axisymmetric Bodies, Wing/Fuselage/Tail, Canard/Wing/Fuselage	2x58 + 4x23=208	Wing/Fuselages	2x58 + 4x23=208	44
Univ. of Southampton, U.K.	TSWT	S	Transonic	FI	-No Tests -		Wings	15x20=300	45

R - Rectangular
S - Square

FI - Flexible, impermeable top and bottom walls.

Table 5

WIAC Systems – 3D Adaptive-Wall Tunnels

					NUMBER OF INTERFACE MEASUREMENTS: # Longitudinal Rows x # Orifices Per Row				
					Full Model		Half Model		
ORGANIZATION	TUNNELS	CROSS SECTION	TEST REGIME	WALL CONFIG	CONFIGURATIONS	NUMBERS	CONFIGURATIONS	NUMBERS	REF.
AEDC Tullahoma,TN	1T	S	High Transonic	All-P,SP	Wing/Fuselage/Tail	(1) 16x40=640	- No Tests -		3
U. of Arizona Tuscon,AZ	AAWT	S	Low Speed, High Lift	B, T-V S-I	Jet-Flapped Wing/Fuselage	4x4 + 4x3 + 2x2=32	- No Tests -		46,47
Tech. Univ. of Berlin, FRG	TUB(3D)	O	Transonic	All-FI	Axisymmetric Body, Wing/Fuselage	6x25 + 2x21=192	- No Tests -		48-51
DFVLR/ Goettingen,FRG	DAM	C	Transonic	FI	Axisymmetric Body Wing/Fuselages Wing/Fuselge/Tail	8x16=128	- No Tests -		50 52-54
NASA/ARC Moffett Field,CA	25cmx13cm	R	Transonic	B,T-S,SPC S-I	- No Tests -		Wing	7x7=49	55
Sverdrup Tech. Tullahoma,TN	AWAT	R	Low Speed, High Blockage, Automotive	T,S-FI,SLS B-I	- No Tests -		Generic Auto	12x18=396	56

R - Rectangular
S - Square
O - Octangular
C - Circular

I - Impermeable, planar walls.
P - Perforated walls.
S - Slotted walls.
V - Ventilated walls w/louvers.

FI - Flexible, impermeable walls.
SP - Segmented porosity.
SPC - Segmented plenum chamber
SLS - Segmented longitudinal strips.

B - Bottom wall.
T - Top wall.
S - Side wall.

(1) Extrapolated from laterally-symmetric case, where 8x40 were used.

x	0.0	0.05	0.1	0.15	0.2	0.25	0.3
R	0.0	0.033	0.045	0.050	0.053	0.055	0.058

x	0.35	0.4	0.45	0.5	0.55	0.6	0.65
R	0.058	0.058	0.058	0.058	0.058	0.058	0.057

x	0.7	0.75	0.8	0.85	0.9	0.95	1.0
R	0.056	0.055	0.052	0.048	0.043	0.038	0.0

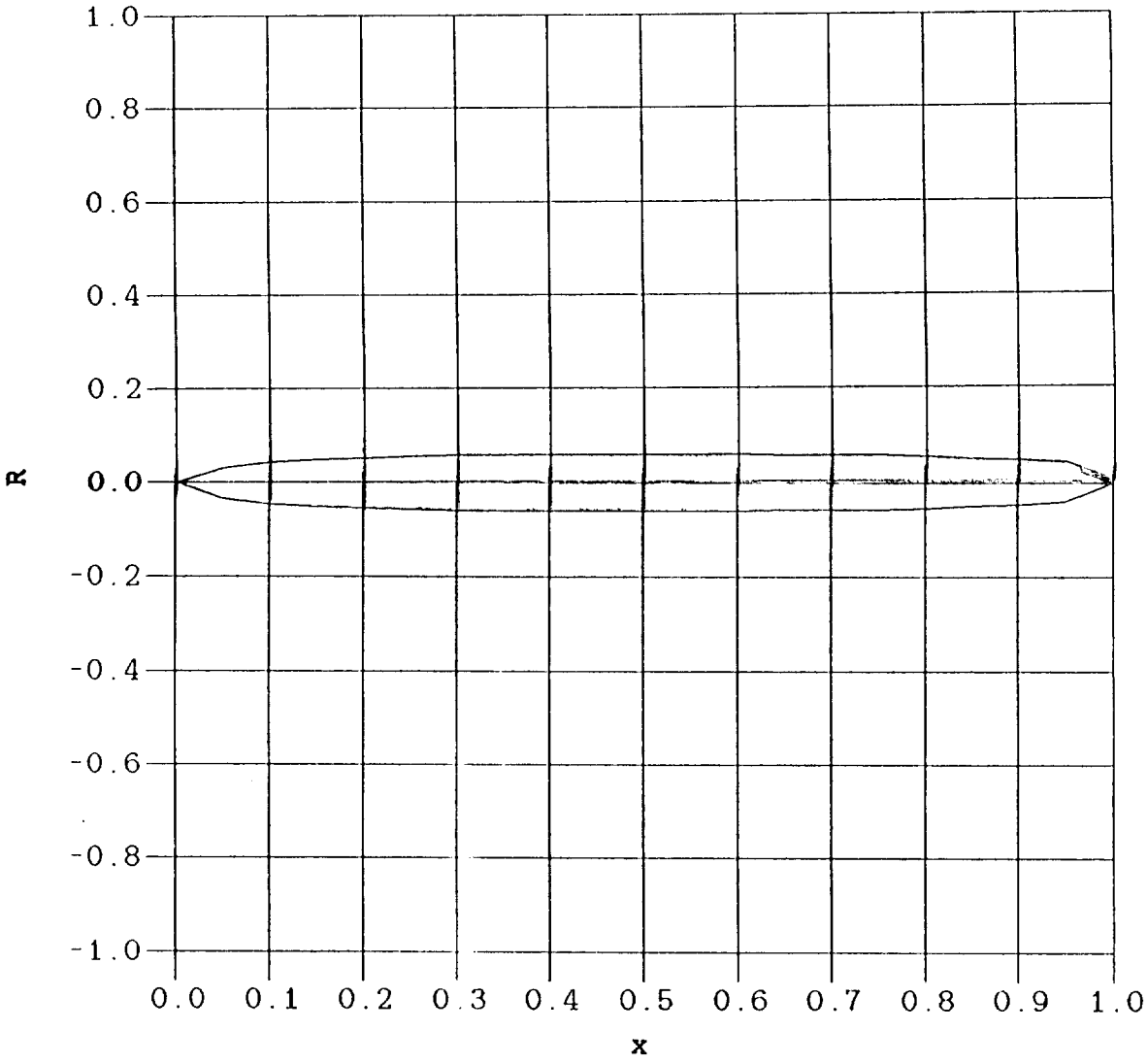

FIGURE 1. ONERA M-5 Body of Revolution Geometry.

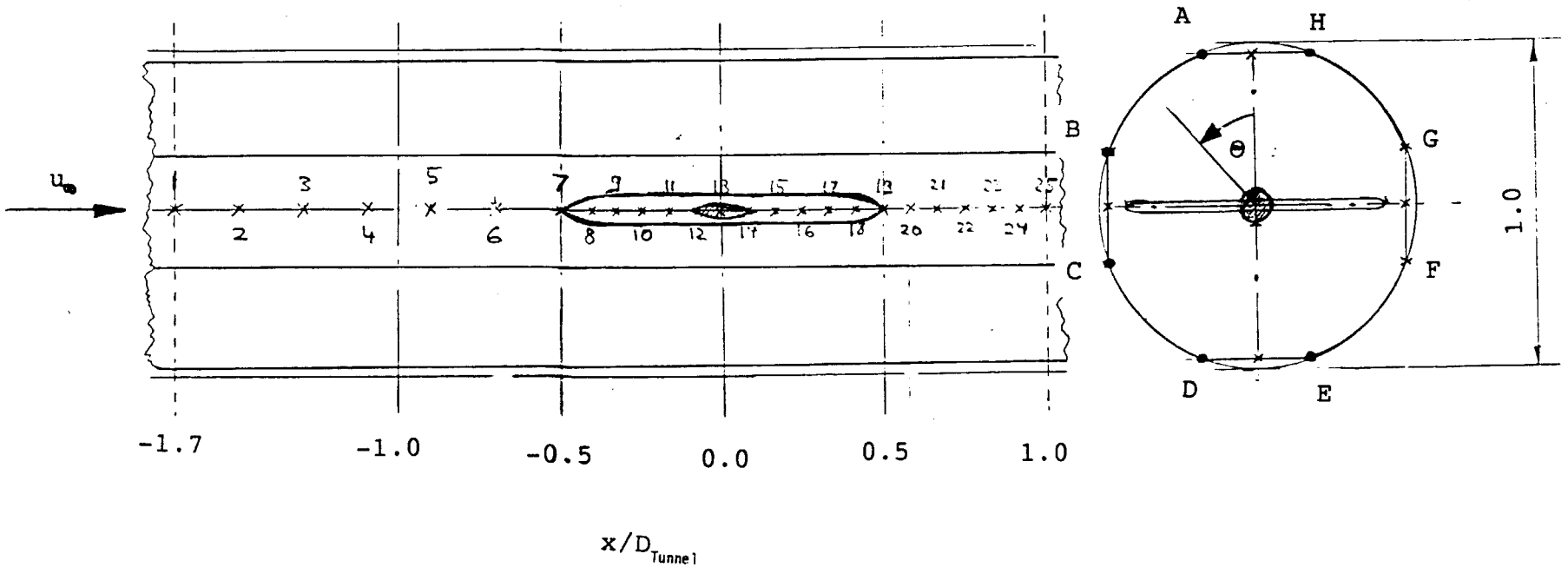

FIGURE 2. Full-Span, Centerline Model Geometry.

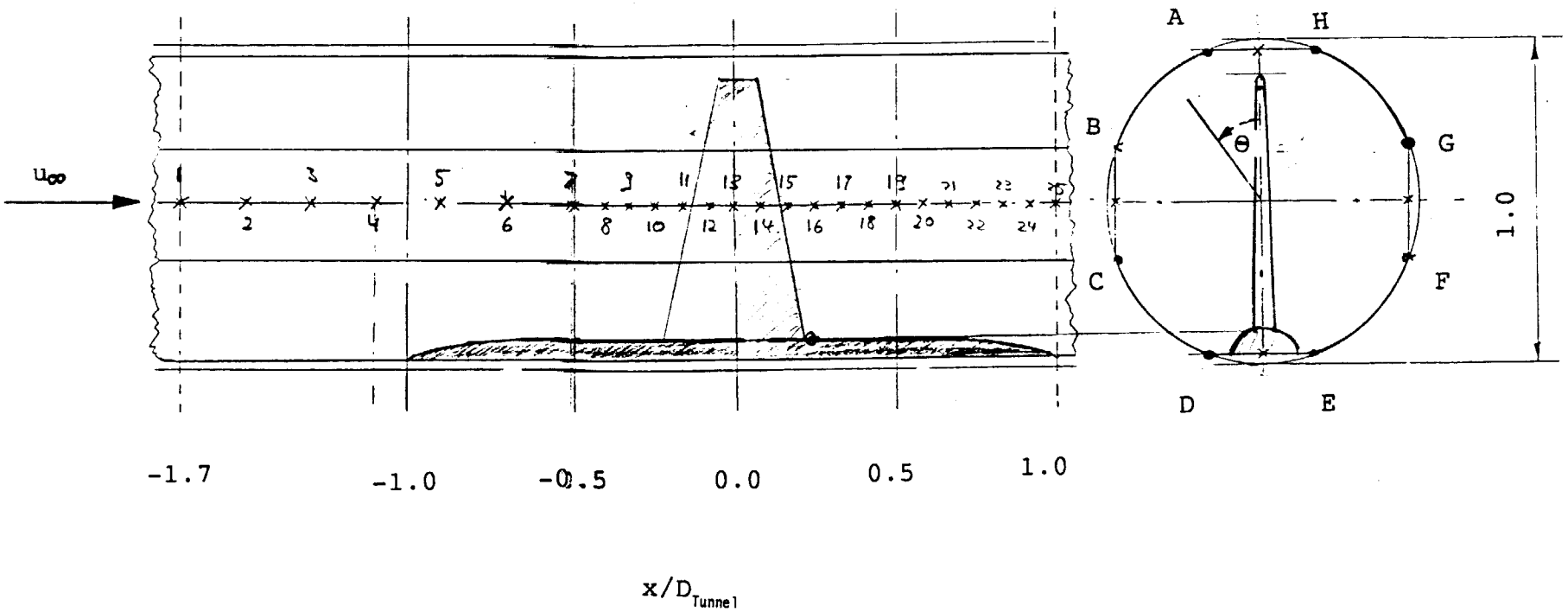

FIGURE 3. Half Model Geometry.

Centerline Model

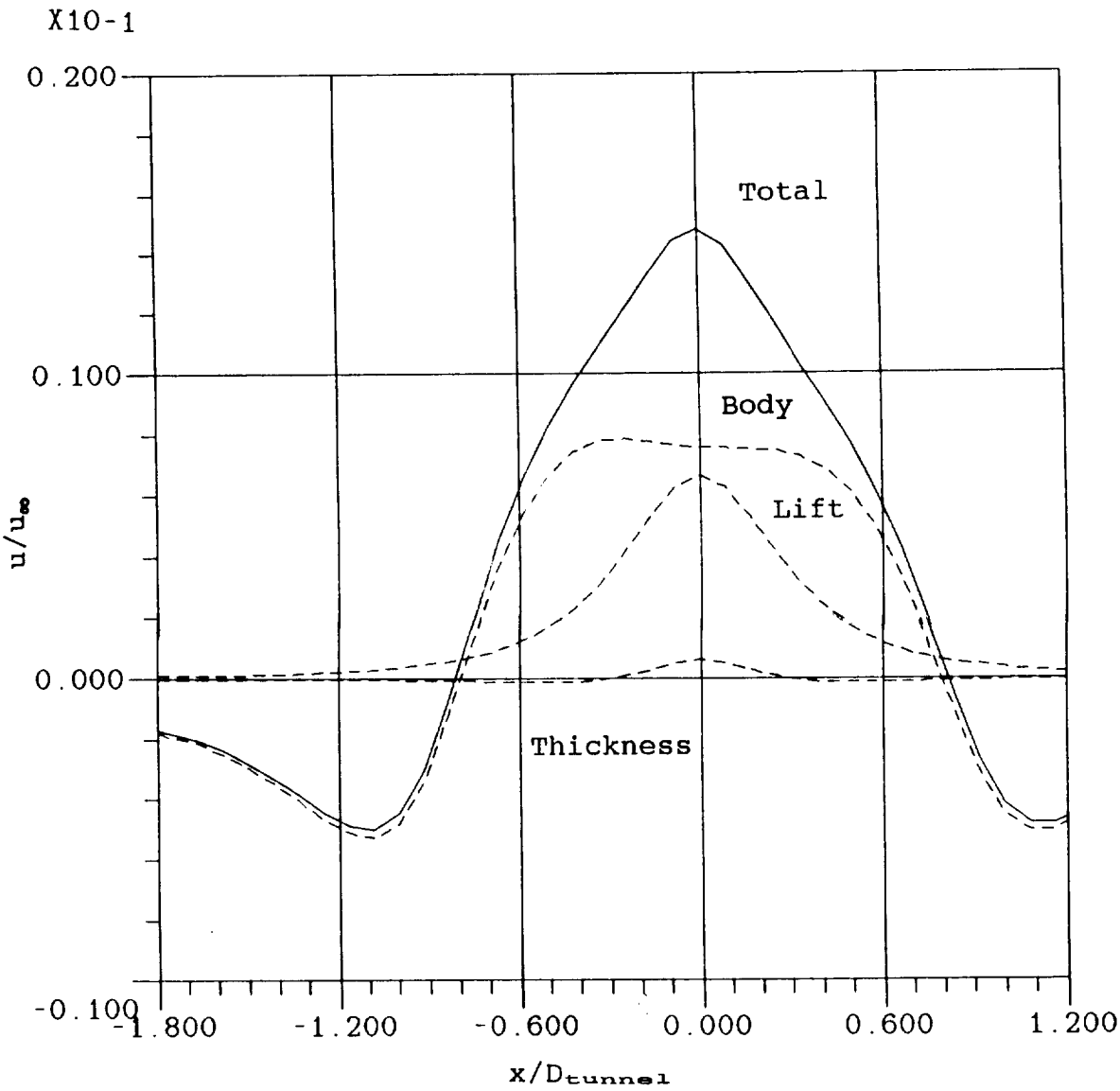

FIGURE 4. Longitudinal Disturbance Velocity Distribution, Θ=20 Deg.

Centerline Model

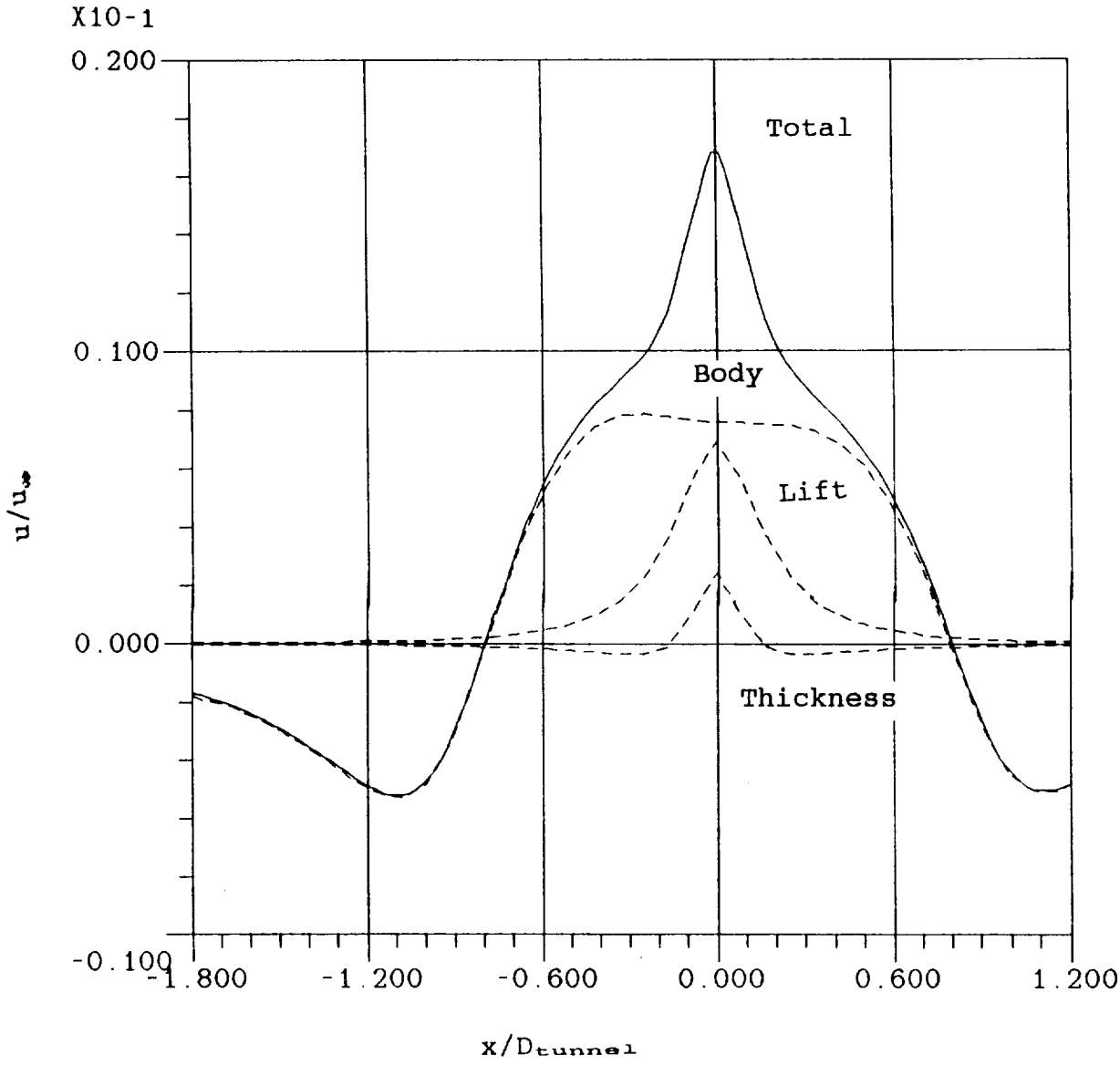

FIGURE 5. Longitudinal Disturbance Velocity Distribution, Θ=70 Deg.

Centerline Model

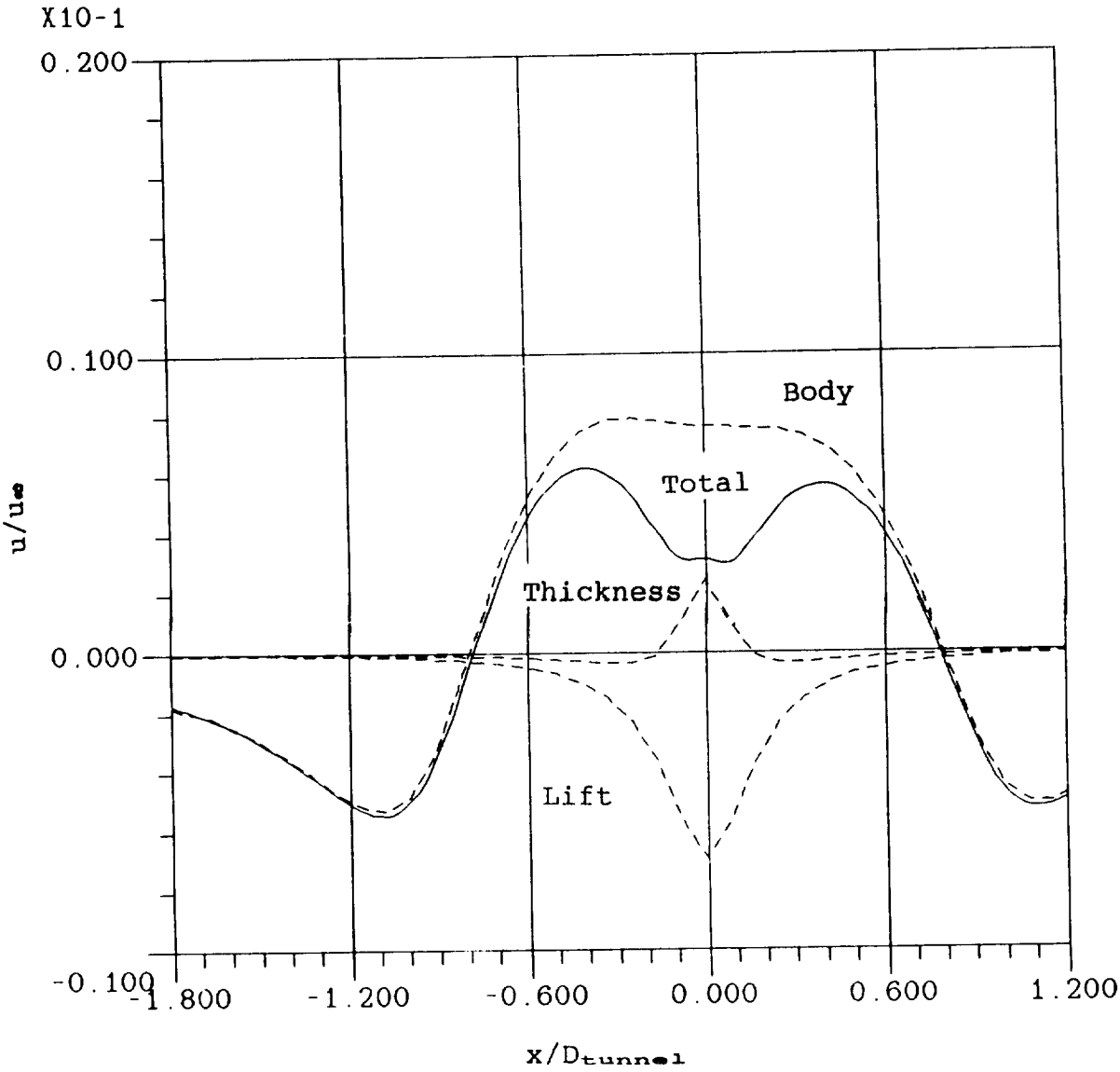

FIGURE 6. **Longitudinal Disturbance Velocity Distribution, Θ=110 Deg.**

Centerline Model

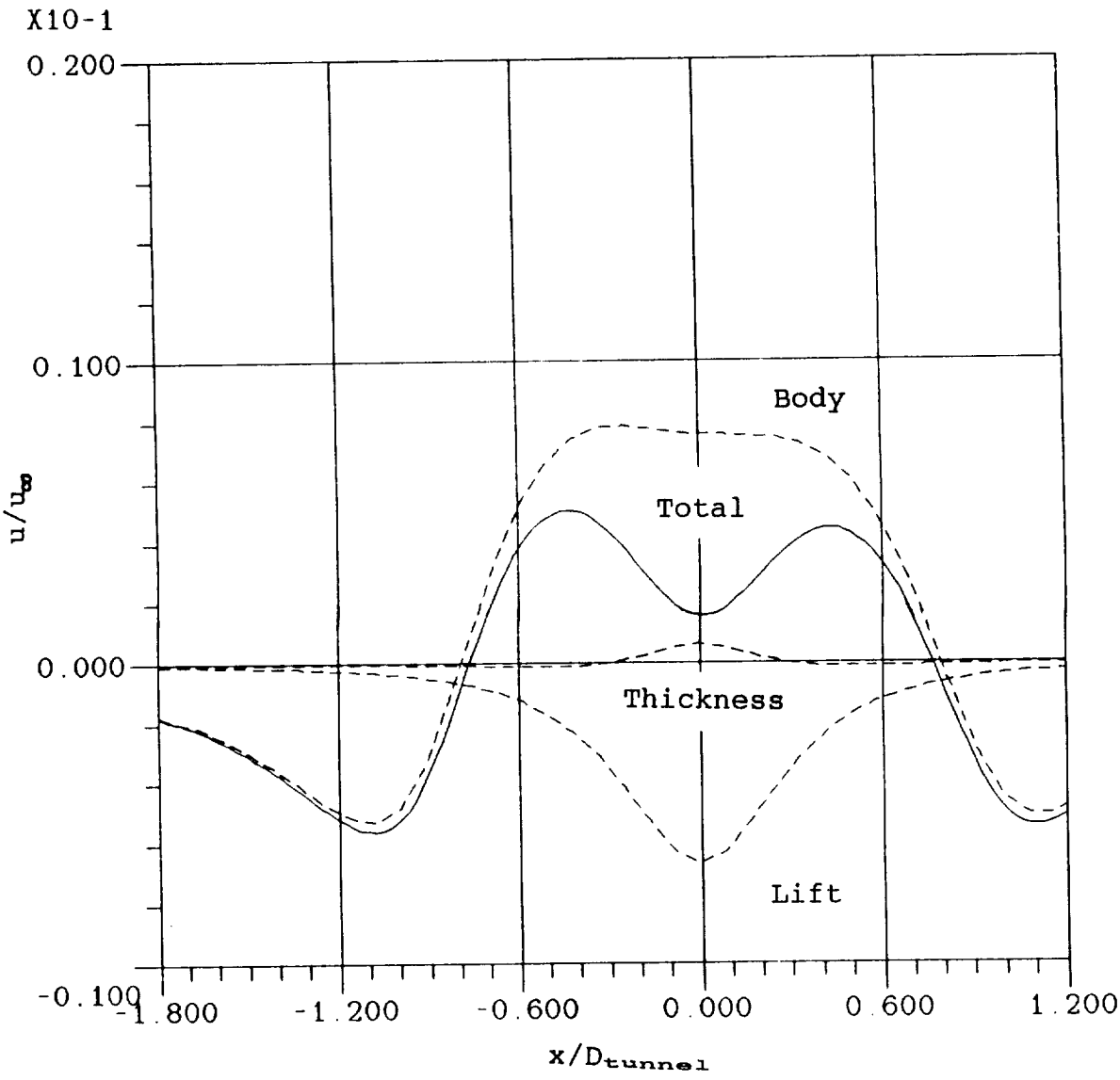

FIGURE 7 **Longitudinal Disturbance Velocity Distribution, Θ=160 Deg.**

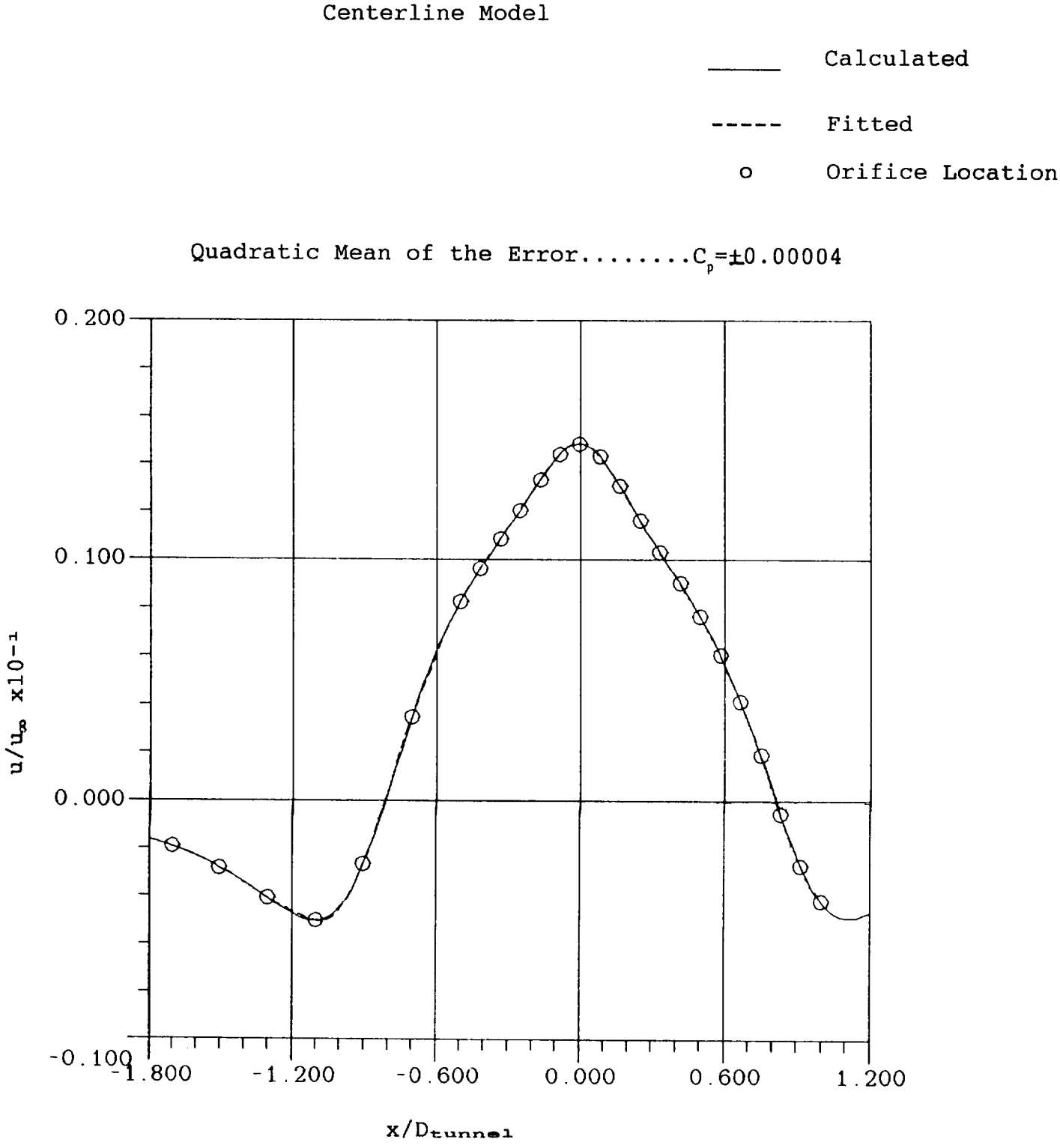

FIGURE 8. **Fitted Disturbance Velocity Distribution, Θ=20 Deg.**

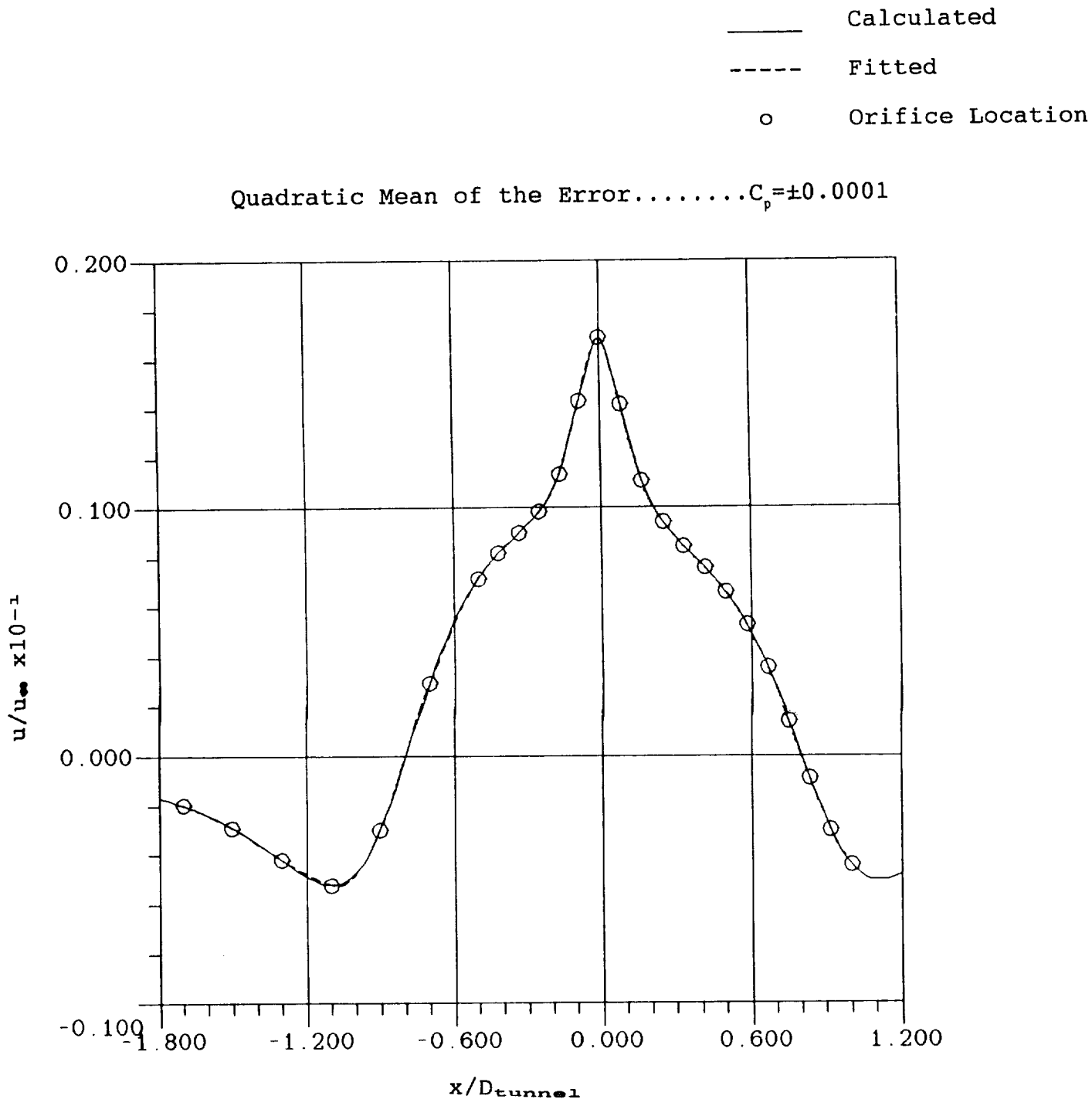

FIGURE 9. **Fitted Disturbance Velocity Distribution, θ=70 Deg.**

Centerline Model

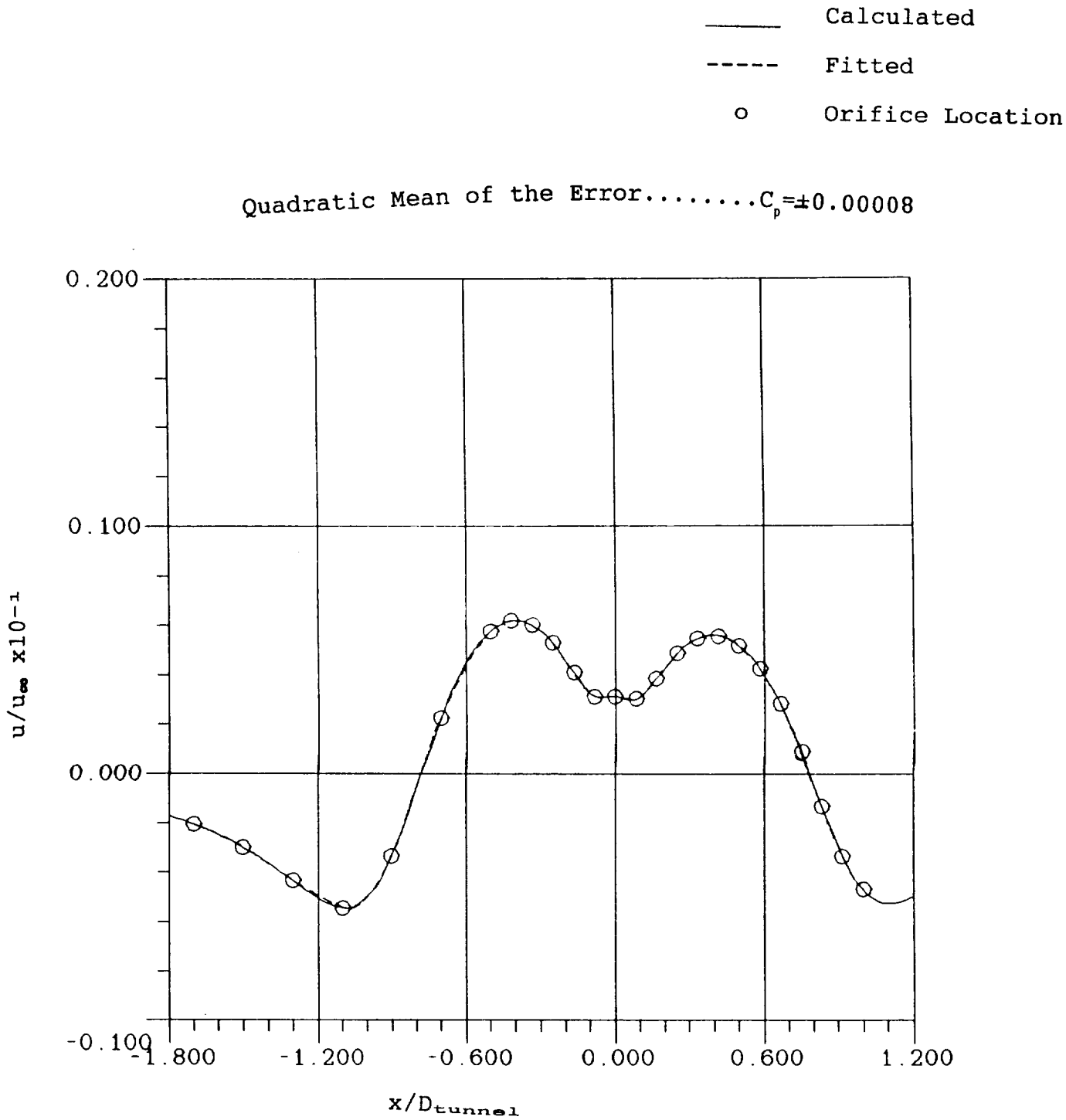

FIGURE 10. Fitted Disturbance Velocity Distribution, θ=110 Deg.

Centerline Model

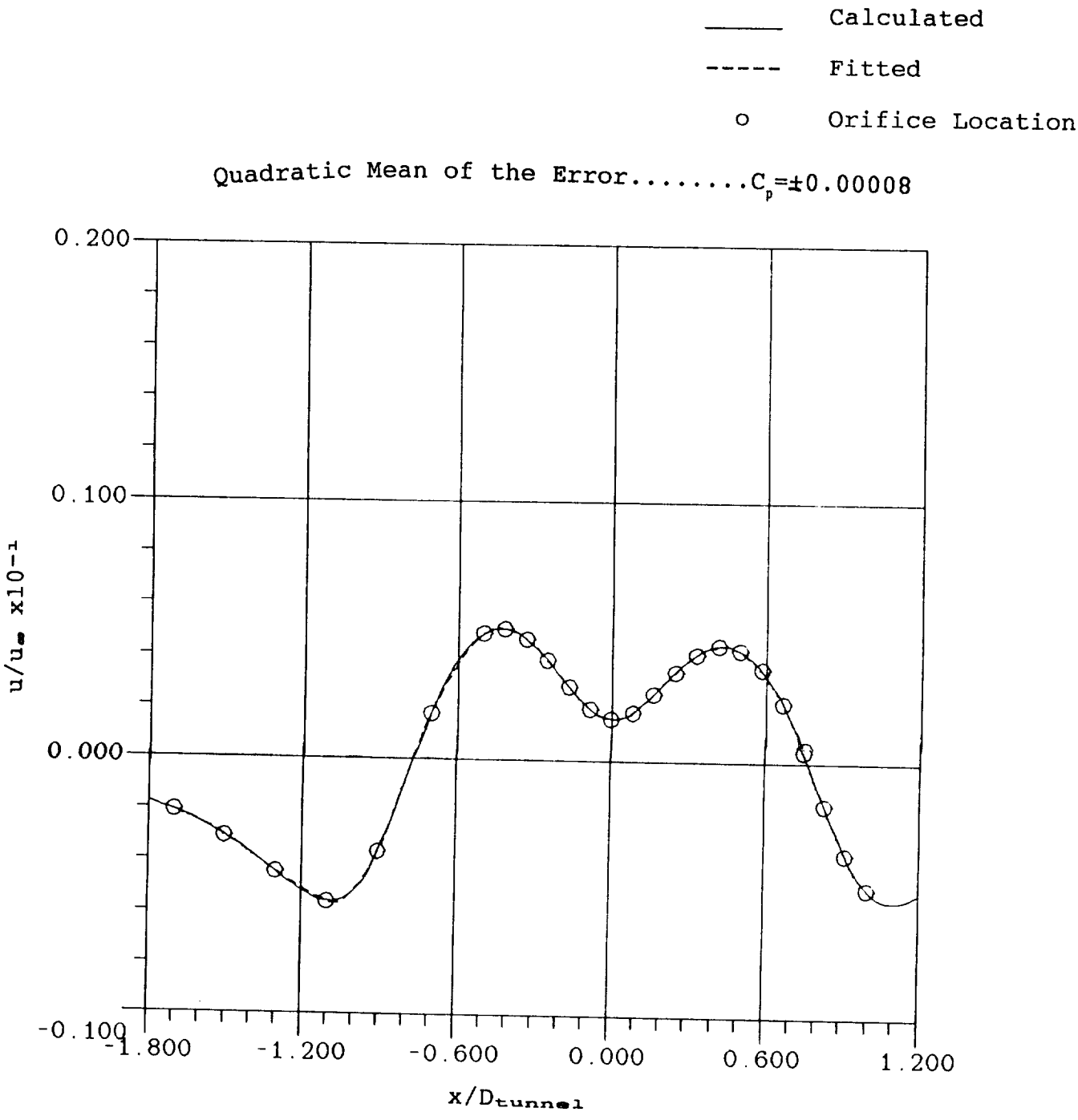

Figure 11 **Fitted Disturbance Velocity Distribution, Θ=160 Deg.**

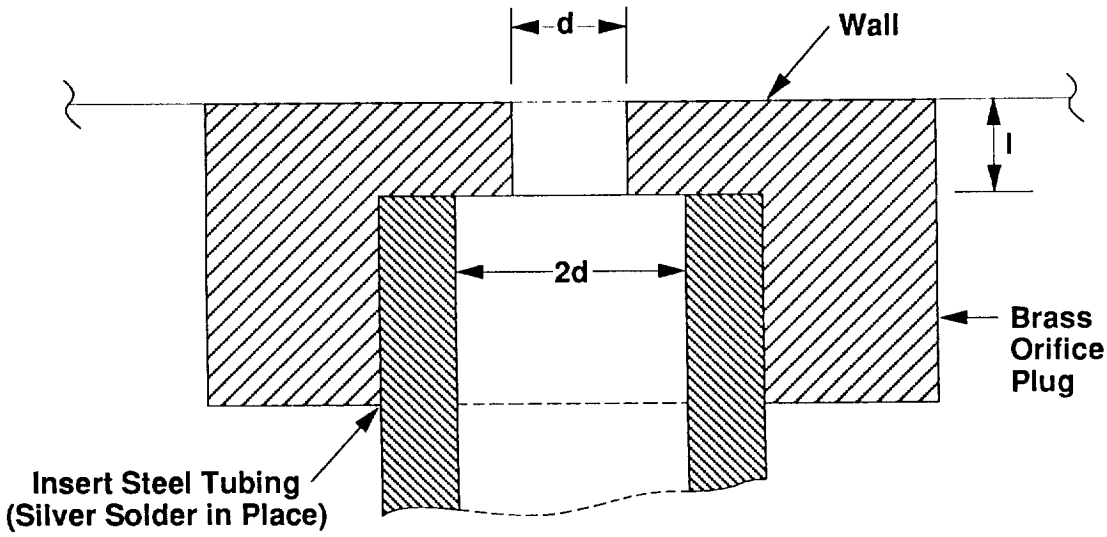

d (orifice Diam.)	0.02 in
l/d	1

1. Plug diameter should match hole diameter to get a force-fit in wall.
2. Pneumatic tubing shall not exceed 20 ft. to maintain small pressure lag time.
3. Orifice shall be square-edged and free from burrs.

FIGURE 12. Static Pressure Orifice Geometry.